




Article

Long-Term Dynamics and Response to Climate Change of Different Vegetation Types Using GIMMS NDVI3g Data over Amathole District in South Africa

Gbenga Abayomi Afuye ^{1,2,*}, Ahmed Mukalazi Kalumba ^{1,2}, Kazeem Abiodun Ishola ^{2,3}
and Israel Ropo Orimoloye ^{2,4,5}

- ¹ Department of Geography and Environmental Science, University of Fort Hare, Private Bag X1314, Alice 5700, Eastern Cape Province, South Africa; akalumba@ufh.ac.za
- ² Geospatial Application, Climate Change and Environmental Sustainability Lab–GACCES, University of Fort Hare, Private Bag X1314, Alice 5700, Eastern Cape Province, South Africa; kazeem.ishola.2018@mumail.ie (K.A.I.); orimoloyeisrael@gmail.com (I.R.O.)
- ³ Irish Climate Analysis and Research Units (ICARUS), Department of Geography, Maynooth University, W23 VP22 Maynooth, Ireland
- ⁴ Centre for Environmental Management, University of Free State, Bloemfontein 9300, Free State Province, South Africa
- ⁵ School of Social Science, The Independent Institute of Education, MSA, Johannesburg 1724, Gauteng Province, South Africa
- * Correspondence: afuyeabayomi@gmail.com



Citation: Afuye, G.A.; Kalumba, A.M.; Ishola, K.A.; Orimoloye, I.R. Long-Term Dynamics and Response to Climate Change of Different Vegetation Types Using GIMMS NDVI3g Data over Amathole District in South Africa. *Atmosphere* **2022**, *13*, 620. <https://doi.org/10.3390/atmos13040620>

Academic Editors: Xiangjin Shen and Binhui Liu

Received: 31 December 2021

Accepted: 20 March 2022

Published: 13 April 2022

Publisher's Note: MDPI stays neutral with regard to jurisdictional claims in published maps and institutional affiliations.



Copyright: © 2022 by the authors. Licensee MDPI, Basel, Switzerland. This article is an open access article distributed under the terms and conditions of the Creative Commons Attribution (CC BY) license (<https://creativecommons.org/licenses/by/4.0/>).

Abstract: Monitoring vegetation dynamics is essential for improving our understanding of how natural and managed agricultural landscapes respond to climate variability and change in the long term. Amathole District Municipality (ADM) in Eastern Cape Province of South Africa has been majorly threatened by climate variability and change during the last decades. This study explored long-term dynamics of vegetation and its response to climate variations using the satellite-derived normalized difference vegetation index from the third-generation Global Inventory Modeling and Mapping Studies (GIMMS NDVI3g) and the ERA5-Land global reanalysis product. A non-parametric trend and partial correlation analyses were used to evaluate the long-term vegetation changes and the role of climatic variables (temperature, precipitation, solar radiation and wind speed) during the period 1981–2015. The results of the ADM's seasonal NDVI3g characteristics suggested that negative vegetation changes (browning trends) dominated most of the landscape from winter to summer while positive (greening) trends dominated in autumn during the study period. Much of these changes were reflected in forest landscapes with a higher coefficient of variation ($CV \approx 15$) than other vegetation types ($CV \approx 10$). In addition, the pixel-wise correlation analyses indicated a positive (negative) relationship between the NDVI3g and the ERA5-Land precipitation in spring–autumn (winter) seasons, while the reverse was the case with other climatic variables across vegetation types. However, the relationships between the NDVI3g and the climatic variables were relatively low ($R < 0.5$) across vegetation types and seasons, the results somewhat suggest the potential role of atmospheric variations in vegetation changes in ADM. The findings of this study provide invaluable insights into potential consequences of climate change and the need for well-informed decisions that underpin the evaluation and management of regional vegetation and forest resources.

Keywords: climate change; dry conditions; NDVI3g; remote sensing; vegetation variability

1. Introduction

Vegetation is an important biophysical factor that controls the terrestrial exchanges of heat, moisture and carbon fluxes between the land and atmosphere, which consequently influences the microclimate through feedback processes at regional scales [1,2]. The vegetation-climate control is achieved through changes in surface albedo and surface

roughness that determines the friction and turbulence, which may vary seasonally and spatially depending on the background climate and plant functional type [3,4]. For instance, grassland typically has a higher surface albedo than the forest ecosystem, suggesting a decrease in transpiration and ultimately leading to cooling or warming depending on which of these processes (e.g., transpiration, photosynthesis and heat exchange) dominates [5,6]. At the same time, vegetation response and growth also depend on subseasonal-to-seasonal changes in local surface and meteorological conditions such as soil moisture which is directly linked to precipitation, temperature, incident solar radiation, etc. For instance, under non-limiting water with the increasing solar radiation and temperature, vegetation responds by opening stomata, thereby enhancing water and carbon uptakes through the processes of transpiration and photosynthesis, respectively and consequently increasing plant productivity [7,8]. The vegetation response and performance also vary across ecosystem types/species [9,10], with changes in biogeochemical cycling across terrestrial ecosystems [11,12]. In the context of climate drivers, temperature, precipitation/soil moisture and incoming solar radiation are the main global climatological drivers of vegetation, whereas if one of these aspects deviates from optimal values, the vegetation becomes stressed and plant productivity declines [13,14]. The resultant deviations, therefore, affect ecosystem functioning and microclimate dynamics. In essence, vegetation plays a pivotal role in global climate, natural resources management, carbon sequestration and ecological biodiversity [15–17].

The evolution of satellite technology has enabled the development of important tools and ecosystem indicators used to monitor vegetation dynamics and trends from regional to global scales. Satellite-derived normalized difference vegetation index (NDVI) is one of such indicators, derived from green leaf scattering in the near-infrared wavelengths (0.72–1.0 μm) and chlorophyll absorption in the red wavelengths (0.58–0.68 μm). Increasing or decreasing the NDVI is considered a reflection of vegetation growth rate, used as an indicator for monitoring seasonal and inter-annual vegetation dynamics, phenological characteristics, land-use change, drought and fire activity, vegetation health and the associated response to climate variations [18–22]. Based on the third-generation Global Inventory Modeling and Mapping Studies (GIMMS; NDVI3g), a study demonstrates a stronger increase in cropland which is further linked to sufficient soil moisture, and a decline in the vegetation trend is linked to the temperature-induced moisture stress in India [23]. Depending on the season, other studies have also attributed increasing the NDVI or vegetation growth to increasing air temperature [24], rainfall variations [21], higher radiation associated with reduced cloud coverage [25] and CO_2 fertilization [26]. In South Africa, a study explored the rainfall–NDVI relationships over a semi-arid wetland in Limpopo Province and reported that vegetation productivity is largely influenced by rainfall variability in this area [27]. Weak to moderate correlations between the NDVI and precipitation and land surface temperature have also been found over Amathole District Municipality (ADM) in Eastern Cape Province [28]. While findings from previous studies provide insight on the potential effects of climate change on vegetation [29], the interactions among climatic variables and how they determine vegetation dynamics across land cover types are still poorly understood, particularly in ADM where climate-related events such as extreme drought often threaten vegetation performance and growth [29].

ADM in Eastern Cape Province of South Africa has witnessed a high record of climate and environment-related degradation such as vegetation stress, water scarcity and dry episodes in the last two decades [30,31]. For instance, ADM was reported to generally receive less than the region's average rainfall amount of 400 mm/year with some few places recording more between 700 and 1000 mm/year occurring in spring and summer months [32,33]. These rainfall variations have effects on the hydrological cycle or water budgets and consequently on the rate of plant growth [34,35]. Hence, the interrelationship between vegetation and climate variables calls for constant monitoring to design appropriate targets to mitigate ecosystem collapse and food security. In essence, the knowledge of vegetation response to climate variations is fundamental to understanding the poten-

tial consequences of climate change in the future. To this end, the remote sensing-based NDVI3g and global reanalyses meteorological variables were explored to investigate the long-term (1981–2015) dynamics and responses to climate change of different vegetation types. The study attempts to answer two basic questions: (i) has the vegetation landscape in ADM experienced a greening or browning trend in the period 1981–2015?; (ii) what is/are the major climatic driver(s) of the response of vegetation types in ADM during this period? These contributions are essential to support the existing knowledge akin to vegetation dynamics and responses of different vegetation types to climate variations and ultimately to inform decision making on degraded areas of vegetation and forest resources.

2. Materials and Methods

2.1. Study Area

ADM in Eastern Cape Province of South Africa is located between $32^{\circ}34'29.99''$ S and $27^{\circ}12'17.40''$ E (Figure 1a), with an elevation of 1963 m. a.s.l. (6440 ft) and a total population of 892,637 [36]. Overall, the district covers a land area of 21,595 km² (8338 sq. mi) with approximately 200 km of coastline [37]. ADM comprises six local municipalities, which include Amahlathi, Ngqushwa, Great Kei, Mquma, Mbashe and Raymond Mhlaba. The district is ranked as the second richest biodiversity in South Africa [38]. This area is characterised by two bio-geographical regions, including the warm temperate south coast and the subtropical east coast [39]. In addition, the land comprises natural areas that are similarly diverse, which include moist mountainous, thornveld, well-watered coastal and semi-arid Karoo and succulent and thicket areas [32,40].

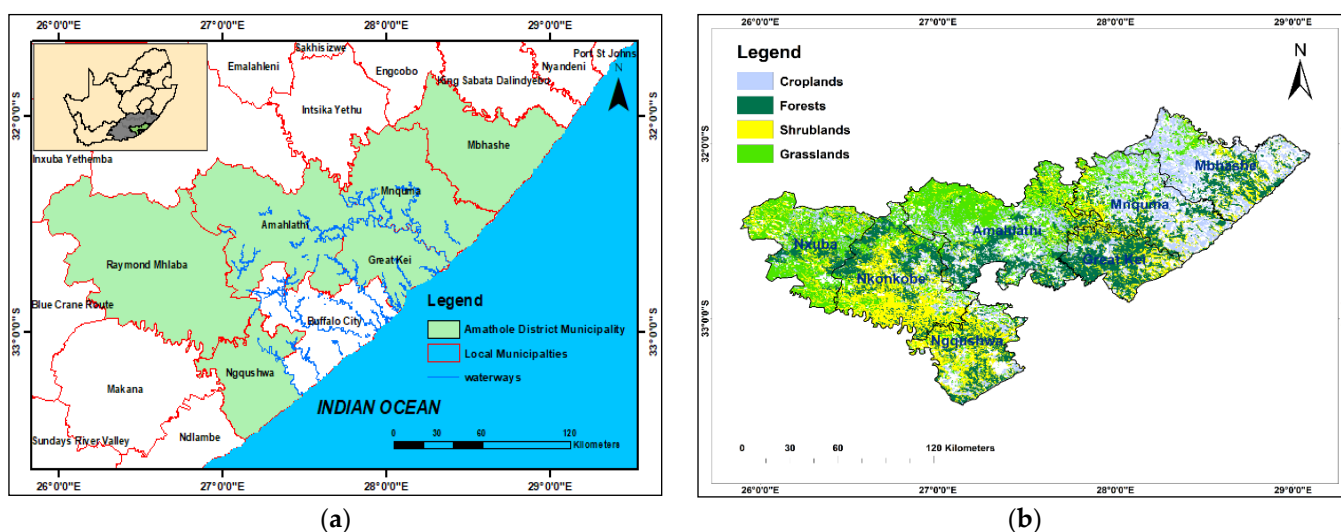


Figure 1. Map showing the local municipalities (a) and the distribution of dominant land cover types (b) in Amathole District Municipality, Eastern Cape Province, South Africa.

In general, a subtropical climate overrides ADM, with rainfall peaking in the summer [41]. The average rainfall is 400 mm/year but fluctuates between 700 and 1000 mm/year in some areas [30,42]. In addition, the average monthly temperature ranges between 1.5 and 2.5 °C and the winter temperature reaching an average of 21 °C, while the summer reaches an average temperature of 28 °C [43]. ADM comprises different eco-topographic undulating grassland and the Amatole mountain range along the Wild Coast from diverse landscape dynamics and climate, which results in various forms of habitats [44,45]. The formation of habitat in ADM varies as a result of the shifting climate and associated influencing factors including soil, topography and vegetation types across the landscape, which are crucial in vegetation distribution.

2.1.1. Satellite-Derived Products

The monthly global GIMMS NDVI3g product was used in this study. The data were obtained from the National Aeronautics and Space Administration (NASA) Ames Ecological Forecasting Lab (<https://ecocast.arc.nasa.gov/data/pub/gimms/3g.v1/>, accessed on 5 July 2021) for the period of 1981 to 2015. The data have a spatial resolution of 0.083° with a 15-day temporal resolution. The products were preprocessed and quality-controlled based on radiometric calibration, atmospheric attenuation, cloud screening, orbital drift, sensor degradation, view and illumination geometry and other effects that are not associated with vegetation change [46,47]. The monthly NDVI3g products are based on the maximum value composite (MVC) method. The MVC selects the highest value of each pixel from multi-temporal data to represent the current NDVI value [48]. For this study, the “Gimms v1.2.1” R package for downloading and processing global GIMMS NDVI3g data was used [49]. Finally, NDVI3g pixels with quality control flag 0 were used in the analysis.

2.1.2. ERA5-Land Reanalysis Data

The ERA5-Land data climate data for ADM were obtained from the Copernicus climate database (<https://cds.climate.copernicus.eu/>, accessed on 7 July 2021) from 1981 to 2015. The climate variables include the 2 m temperature ($^\circ\text{C}$), precipitation (mm), wind speed (m/s) and shortwave radiation downwards (W/m^2). The data are available hourly and at temporal and spatial resolutions of 0.01° and 0.01° , respectively. The global reanalysis ERA5-Land is the fifth generation global reanalysis product from the European Center for Medium-Range Weather Forecast (ECMWF) and supersedes its predecessors [50,51].

2.1.3. Ancillary Data

The land cover data for ADM were obtained from Copernicus Climate Data Store (<https://cds.climate.copernicus.eu/>, accessed on 7 July 2021) for 1992 and 2015. The data for both years were compared in a logical approach to remove pixels or land cover that have been modified or changed due to urbanization, deforestation, agricultural practices, etc. over the 23 years [52]. The stable pixels over the years were subsequently retained for analysis in this study. The retained stable pixels were reclassified by grouping the major land covers in ADM into four types, namely grassland, cropland, forest and shrubland, which means that these four types at both dates were taken to establish a mask for different land cover types (Figure 1b). The land cover maps were generated by the European Space Agency Climate Change Initiative (ESA CCI) [53]. The global land cover maps were produced at a spatial resolution of 300 m. Finally, all the data were harmonised from their native resolutions into common spatial (0.083°) and temporal (monthly) resolutions before analysis.

2.2. Study Methods

First, spatial, seasonal and inter-annual characteristics of NDVI3g were analysed. For seasonal analysis, the entire period was characterised into four seasons, which included winter (June, July and August), spring (September, October and November), summer (December, January and February) and autumn (March, April and May). The long-time climatology, trend and coefficient of variation (CV) of NDVI3g and climate variables were subsequently calculated for each season and vegetation type. The NDVI values typically range from about -0.2 to 0.1 for inland water bodies, snow, deserts, bare soils and sparsely vegetated areas and from 0.1 to 1 for increasing amounts of vegetation.

2.2.1. Coefficient of Variation

The coefficient of variation (CV) is generally used in vegetation studies and is mainly used to reflect the discrete degree of the NDVI data and the inter-annual variability of vegetation [54,55]. The CV was estimated as following:

$$CV_{\text{NDVI}} = \frac{\mu_{\text{NDVI}}}{\delta_{\text{NDVI}}}, \quad (1)$$

where CV_{NDVI} denotes the CV of the seasonal NDVI values of each pixel from 1981 to 2015; δ_{NDVI} is the standard deviation of the seasonal NDVI values for 1981–2015; μ_{NDVI} is the long-term mean seasonal NDVI value. A higher CV_{NDVI} value indicates that the NDVI time series shows a higher data variation, while a lower CV_{NDVI} indicates a more stable NDVI time series.

2.2.2. Trend Analysis

The trend in NDVI3g and climate variables were analysed using the non-parametric Mann-Kendall test [56,57]. The method has been widely used to identify trends and climate and vegetation series [58–60]. For the trend analysis, the confidence intervals were expressed using the Mann-Kendall static (M):

$$M = \sum_{i=1}^{n-1} \sum_{j=i+1}^n sgn(y), \tag{2}$$

where n is the length of time series data and $y = P_j - P_i$; $sgn(y)$ is estimated as:

$$sgn(y) = \begin{cases} 1, & \text{if } y > 0 \\ 0, & \text{if } y = 0 \\ -1, & \text{if } y < 0 \end{cases} . \tag{3}$$

The negative and positive differences in data samples are represented by statistics. For the null hypothesis, the mean of M is zero, i.e., $E(M) = 0$, and the variance, σ , was expressed as:

$$\sigma = \frac{n(n-1)(2n+5) - \sum_{j=1}^n (t_j-1)(2t_j+5)}{18}, \tag{4}$$

where t_j is the size of any given j th tie. The M test statistic distribution is subject to Z -transformation, which was described as:

$$Z = \begin{cases} \frac{M-1}{\sqrt{\sigma}}, & M > 0 \\ 0, & M = 0 \\ \frac{M+1}{\sqrt{\sigma}}, & M < 0 \end{cases} . \tag{5}$$

The ‘‘Sen’’ slope’s magnitude [61] was estimated as the median overall values of the entire data and expressed as:

$$S_k = Median\left(\frac{P_j - P_i}{j - i}\right), \text{ for } (1 \leq i < j \leq n), \tag{6}$$

where P_j and P_i represent data values at times j and i ($j > i$), respectively, while n is the number of data. A positive (negative) slope indicates an upward (downward) trend.

2.2.3. Partial Correlation Analysis

To understand the relationship between vegetation and climate variables across ADM, pixel-wise partial correlation analysis was carried out between the NDVI3g and each climate variable for each season and the land cover type, for the period 1981–2015 [62–64]. The partial correlation coefficients between variables can be expressed as:

$$R_{ab,c,d,e} = \frac{r_{ab} - r_{ac}r_{ad}r_{ae}r_{bc}r_{bd}r_{be}r_{cd}r_{ce}r_{de}}{\sqrt{1 - r_{ac}^2} \sqrt{1 - r_{ad}^2} \sqrt{1 - r_{ae}^2} \sqrt{1 - r_{bc}^2} \sqrt{1 - r_{bd}^2} \sqrt{1 - r_{be}^2} \sqrt{1 - r_{cd}^2} \sqrt{1 - r_{ce}^2} \sqrt{1 - r_{de}^2}}, \tag{7}$$

where $R_{xy,z,i}$ is the partial correlation coefficients between variables a (NDVI3g product) and b (e.g., precipitation) while controlling the remaining variables c, d, e ; r is the Pearson correlation coefficient between variables x and y , between x and z , or between y and z for product i .

3. Results

3.1. Spatial and Temporal Variations in Vegetation across ADM

The study assessed spatiotemporal variations in the NDVI3g across Amathole District during the period from 1981 to 2015. The analysis of the NDVI3g climatology indicated that there was no distinct difference in vegetation characteristics across the seasons (Figure 2). However, for spatial characteristics, the values of NDVI3g increased from approximately 0.3 in the northern and western fringes to 0.8 in the southeastern part of ADM. The areas with low NDVI3g values were majorly dominated by grass and/or shrubs, while areas with high NDVI3g values were characterised by forest cover and/or crop landscape (Figure 1b).

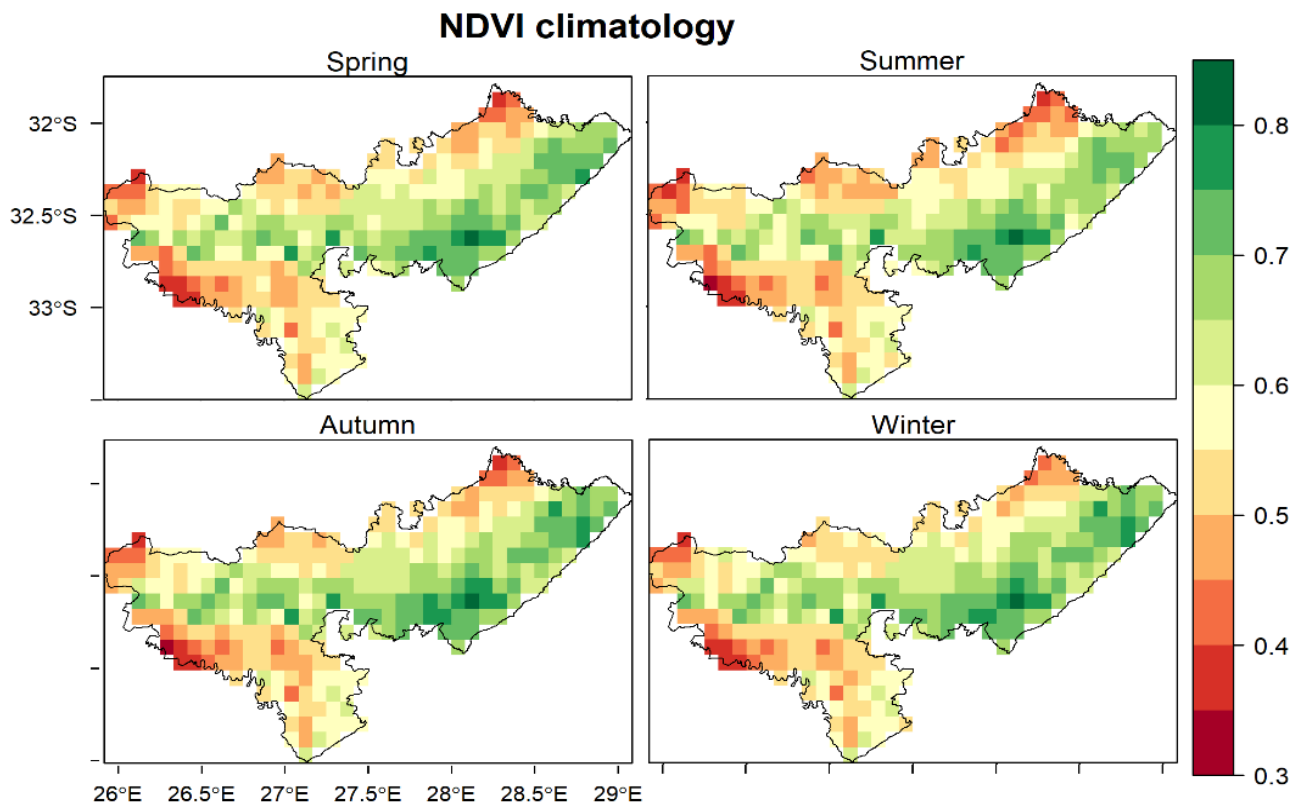


Figure 2. Spatial and seasonal characteristics of third-generation Global Inventory Modeling and Mapping Studies (NDVI3g climatology) (1981–2015) for Amathole District Municipality.

The spatial trend in the NDVI3g for each season is shown in Figure 3. For the analysis period, the results indicated decreasing (browning) trends of NDVI3g across a wider part of ADM in spring (September, October and November), summer (December, January and February) and winter (June, July and August), except over grass landscapes in which the NDVI3g showed significant (p -value < 0.05) increasing (greening) trends in spring and winter. In autumn, the NDVI3g also showed significant increasing trends largely across the entire landscape. Overall, the trends in the NDVI3g were weak across the landscapes and seasons.

The boxplots (Figure 4) showed the long-term CV of the NDVI3g (CV_{NDVI}) across seasons and vegetation types. Again, the variations of the NDVI3g were uniform (mean $CV_{NDVI} \approx 10$) across the seasons and vegetation types, except for forest landscapes, which showed higher changes (mean $CV_{NDVI} \approx 15$) in the NDVI3g across seasons, for the analysis period.

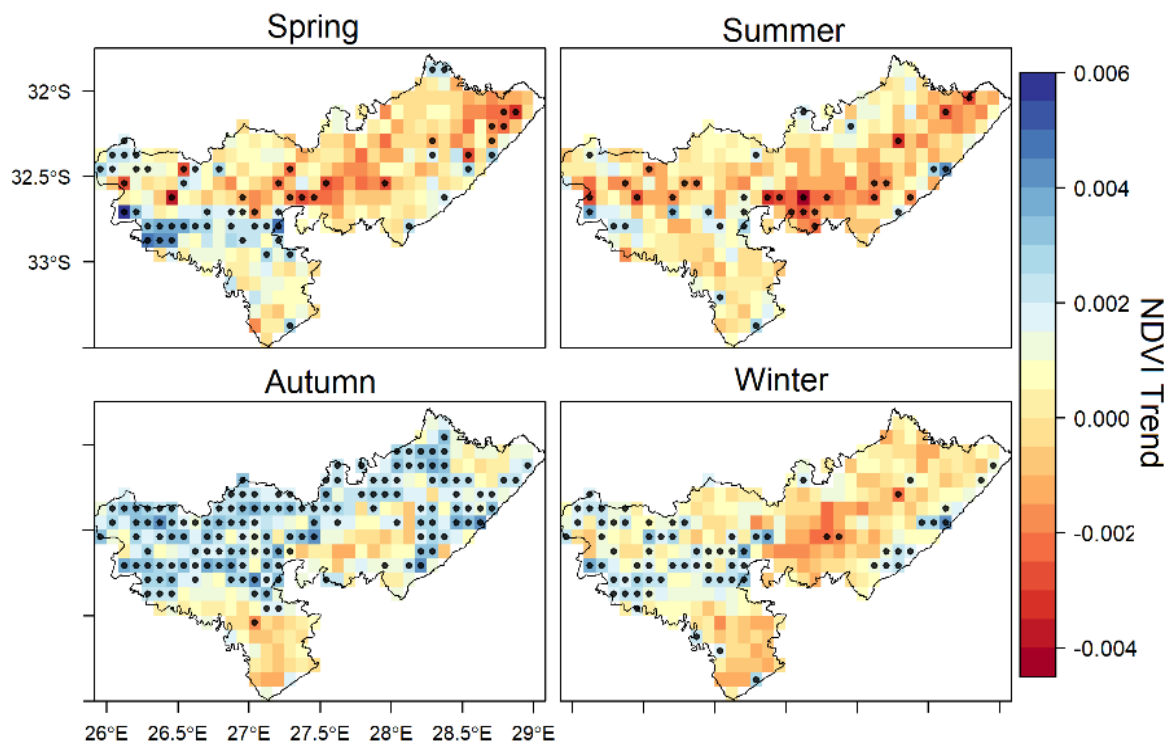


Figure 3. Spatial trends in the NDVI3g across the seasons for Amathole District Municipality. The stippling indicates pixels with statistical significance (p -value < 0.05).

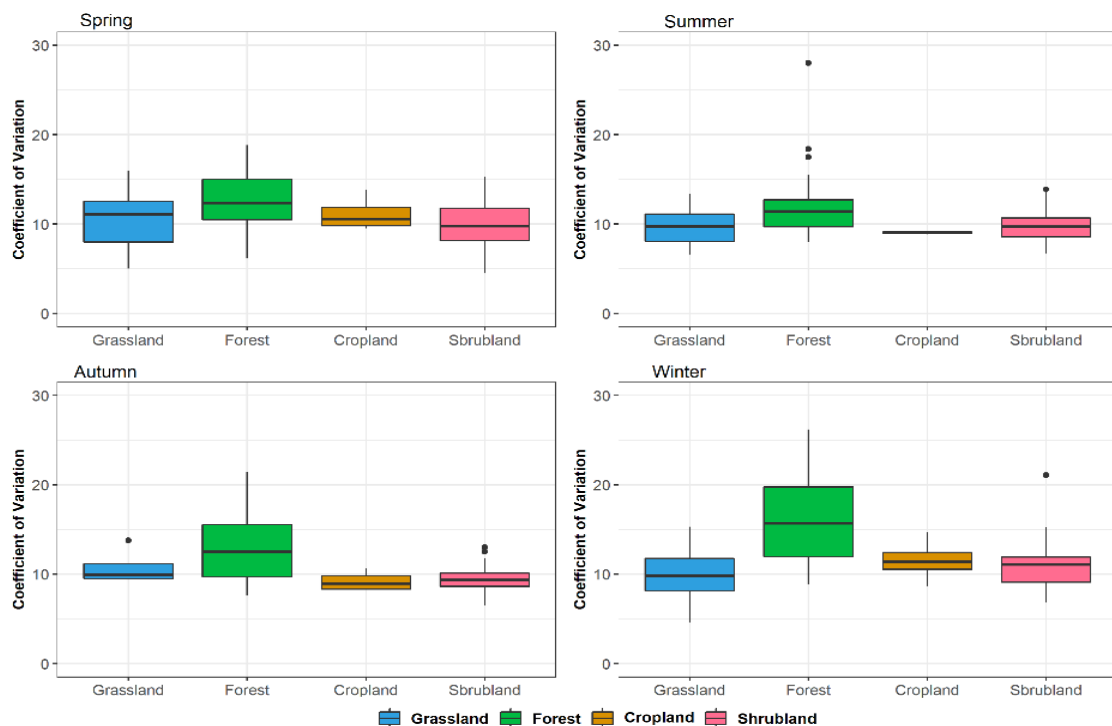


Figure 4. Coefficients of variation of the seasonal NDVI3g during 1981–2015 for different vegetation types for Amathole District Municipality.

3.2. Relationship between Vegetation and Climatic Variables

3.2.1. NDVI3g and Air Temperature

The pixel-wise partial correlation coefficients between the NDVI3g and the ERA5-Land temperature across the region are presented in Figure 5. The results showed negative

correlations between the NDVI3g and the air temperature, majorly in the northeast in winter and spring. In summer, the negative correlations covered a wider part of ADM, and it occupied a much larger part, in autumn. The boxplot shows the upper and lower quartiles ranges with different classes of vegetation types in ADM. Specifically, the negative correlations ($R \approx 0.2$) were dominated over croplands and forests in winter and spring. All vegetation types show a negative relationship with the air temperatures in summer and autumn, but stronger ($R > 0.2$) over grasslands and shrublands, relative to forests and croplands during these periods. These results are counter-intuitive, because vegetation growth is expected to increase with the rising temperature normally in the course of a growing season (spring–autumn). However, an extremely high temperature above the optimum for vegetation growth may induce vegetation stress in association with the rising soil moisture deficit [23]. Interestingly, the trends in ERA5Land air temperature show somewhat an increase over the analysis period, particularly from winter to summer (Figure S1). This suggests that air temperature could potentially drive vegetation changes during this period. Generally, the correlations between the NDVI3g and the ERA5-Land air temperature were low ($R < 0.4$) and largely insignificant across the seasons, particularly in spring and summer, and vegetation types.

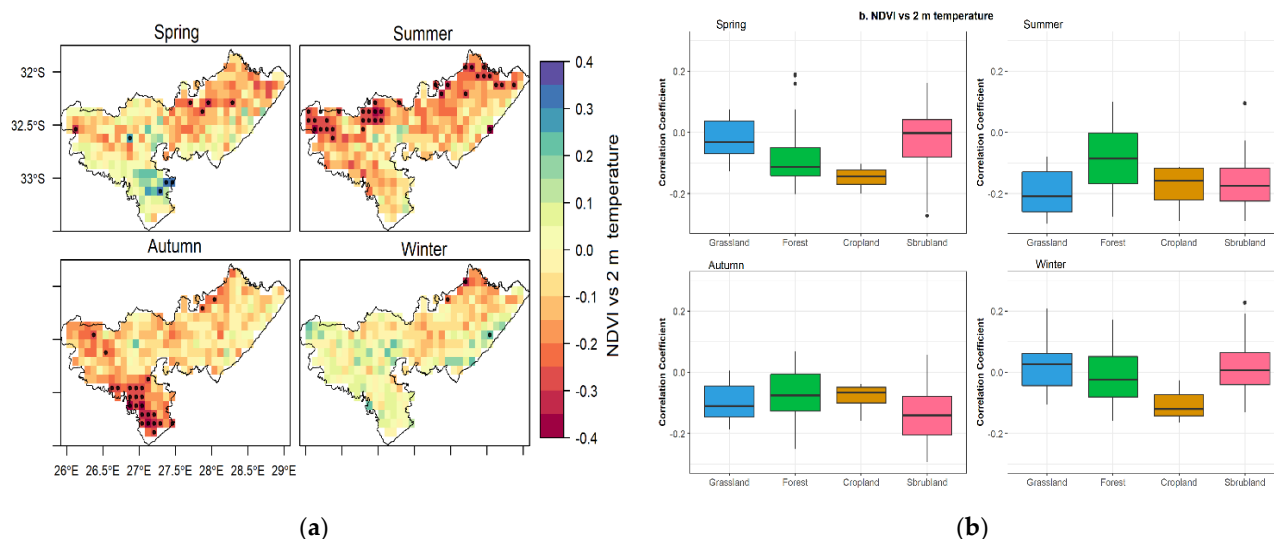


Figure 5. (a) Pixel-wise partial correlation coefficients between the NDVI3g and the ERA5-Land 2 m temperature for Amathole District Municipality; and (b) boxplots of the correlation for vegetation types. The stipplings are for pixels with statistical significance (p -value < 0.05).

3.2.2. NDVI3g and Precipitation

The pixel-wise partial correlation coefficients between the NDVI3g and the ERA5-Land precipitation across the region are presented in Figure 6. The NDVI3g showed a positive correlations ($R > 0.25$) with precipitation during spring–autumn across the landscapes, except for a few isolated areas dominated by forests where the correlations were negative. In winter, the correlations ($R > 0.3$) were negative, largely over the entire domain. In the context of vegetation types, the positive correlations were more dominated over forests and shrubs in spring and over all vegetation landscapes except forests in summer and autumn. In winter, negative relationships occurred over all the vegetation types, except croplands. Concurrent with the NDVI3g, the ERA5-Land precipitation trends showed that precipitation decreased insignificantly in many areas from autumn to spring over the analysis period (Figure S2). However, the correlation results, which were also statistically insignificant, suggested that precipitation is less an important driver of long-term vegetation dynamics in ADM.

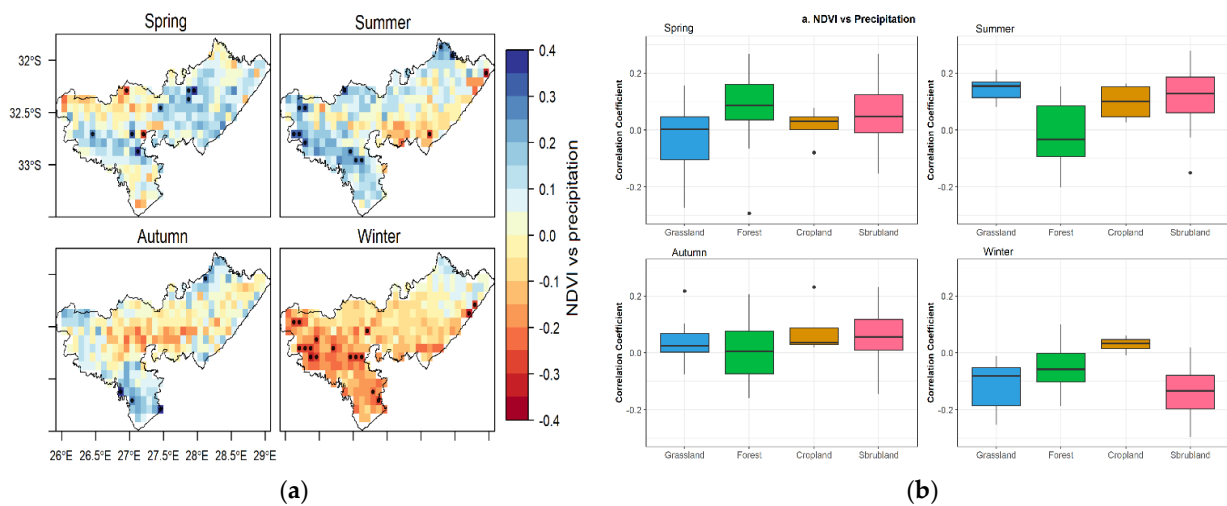


Figure 6. (a) Pixel-wise partial correlation coefficients between the NDVI3g and the ERA5-Land precipitation for Amathole District Municipality; and (b) boxplots of correlation for vegetation types. The stipplings are for pixels with statistical significance (p -value < 0.05).

3.2.3. NDVI3g and Incoming Shortwave Radiation

The pixel-wise partial correlation coefficients between the NDVI3g and the ERA5-Land shortwave radiation across the region are presented in Figure 7. The correlation results were nearly similar to the NDVI3g vs. the air temperature (see Section 3.2.1 and Figure 5). This is anticipated, since the incoming shortwave radiation was linearly related to air temperature. In essence, a rise in the incident radiation would imply an increase in the air temperature and vegetation growth in an ideal situation. Figure 7 shows that the negative correlations ($R > 0.2$) between the NDVI3g and the radiation were mostly dominated over shrubs and forests in spring while shrubs and grasslands retain the negative correlations in summer. In autumn, all the vegetation types showed a negative correlation with the radiation, with shrubs indicating the strongest ($R > 0.3$). In contrast, the NDVI3g were positively related to the radiation ($R \approx 0.1$ – 0.2) over all the vegetation types in winter. These results reflected the insignificant positive trends in shortwave radiation (Figure S3) in spring and, to some extent, in summer, in contrast to negative trends in the NDVI3g during these seasons (see Figure 3). Generally, the correlation values were also weak ($R < 0.4$) and largely insignificant across ADM during the analysis period.

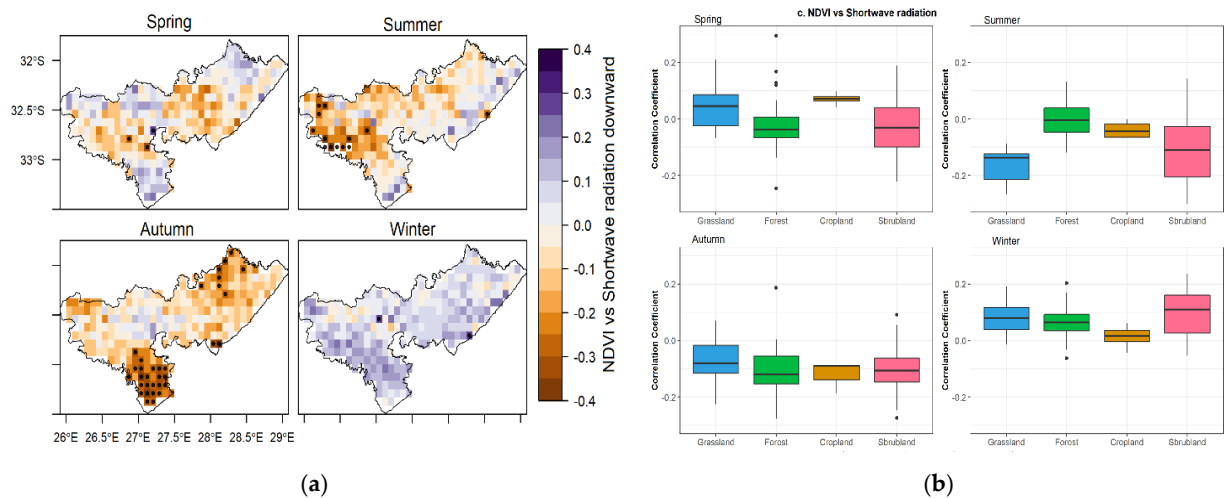


Figure 7. (a) Pixel-wise partial correlation coefficients between the NDVI3g and the ERA5-Land shortwave radiation downward for Amathole District Municipality; and (b) boxplots of correlation for vegetation types. The stipplings are for pixels with statistical significance (p -value < 0.05).

3.2.4. NDVI3g and Wind Speed

The pixel-wise partial correlation coefficients between the NDVI3g and the ERA5-Land wind speed across the region are presented in Figure 8. The correlations between the NDVI3g and the wind speed were negative, majorly over forests and shrubs in the south of ADM in spring. In summer and autumn, the entire domain was dominated by negative correlations ($R > 0.2$), while in winter, all the vegetation landscapes showed positive correlations with the wind speed. Similar to other climatic variables, the relationship between the NDVI3g and the ERA5-Land wind speed was generally weak and largely insignificant. Nonetheless, the negative correlation results are consistent with the results of trends in the wind speed (Figure S4) and the NDVI3g (Figure 3).

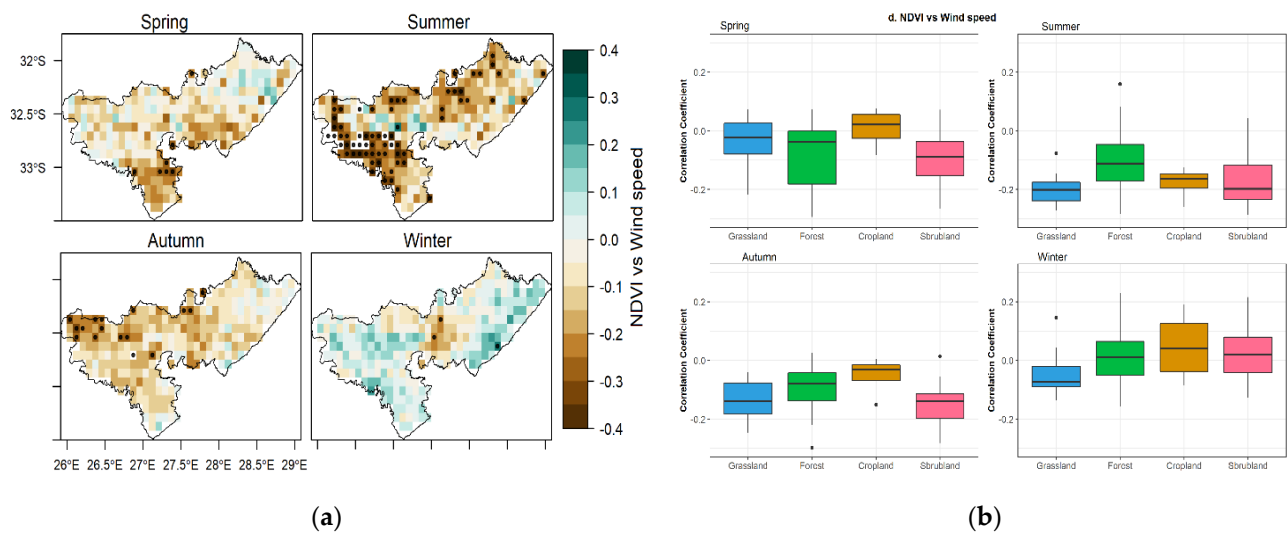


Figure 8. (a) Pixel-wise partial correlation coefficients between the NDVI3g and the ERA5-Land wind speed for Amathole District Municipality; and (b) boxplots of correlation for vegetation types. The stipplings are for pixels with statistical significance (p -value < 0.05).

4. Discussion

The results from this study revealed spatial and seasonal characteristics of the NDVI3g climatology and trend for different climate variables across ADM from 1981 to 2015. The climate variables exhibited a seasonal variation from one season to another during the study period. The results of negative correlations between NDVI3g and climate variables in the region might have significant implications on the hydrological cycle, human and livestock health and nutrition as well as ecosystem functioning. For instance, the variations in rainfall distribution in ADM might pose negative threats to food security, water availability and plant growth which may lead to recurrent droughts that are exacerbated by climate change. In the Northern Hemisphere, NDVI is largely influenced by temperature which connotes that a rising temperature/radiation implies an increase in vegetation activities [6,26]. Moreover, in a semi-arid environment, particularly in ADM where declining precipitation was observed in many areas, suggesting that precipitation is less an important driver of vegetation dynamics in the region. The declining precipitation and rising temperature are likely to have contributed to the drying trends and the resultant observed vegetation activity in the region. Therefore, it is important to recognise heterogeneous vegetation landscape characteristics and climate in ADM associated with the environment-related effect on vegetation cover. In essence, the major climatic drivers of the response of vegetation types can help to improve our understanding of vegetation landscapes and their impacts on a local scale as well as regional climatic conditions. Depending on land heterogeneity, the response of vegetation change has an impact on the regional circulation pattern, resulting in the various responses of climatic variables [65,66]. The seasonal characteristics of the NDVI3g climatology in ADM revealed a high spatial heterogeneity in vegetation growth

trends. Although the overall vegetation-covered areas in ADM have been growing, the increase of the spatial heterogeneity in vegetation change trend requires management and development planning.

The CV of the seasonal NDVI3g vs. temperature, precipitation, solar radiation and wind speed yielded time-dependent NDVI characteristics for each vegetation type. This quantifies the NDVI3g trends in relation to the dynamic effects of individual variables contributing to the spatial variability of forest, grassland, shrubland and cropland across ADM. The results showed evidence of the areas with high NDVI3g values characterised by forest cover and crop landscape and areas with low NDVI3g, where grassland and shrubland showed the highest productivity for different seasons. Based on the findings of this study, positive and negative correlations of vegetation with climatic variables were observed across landscapes and seasons, which suggested negative vegetation changes (browning trends) dominated most of the landscape from winter to summer while positive (greening) trends dominated in autumn during the study period. Overall, the trends in the NDVI3g were weak across the landscapes and seasons, which might be attributed to the semiarid microclimate dynamics of the region. This connotes that climate characteristics in large areas are more complex and changeable than those in microscale areas, because the climates vary significantly at the microscale level than those in large-scale areas with varying influences on vegetation dynamics [10,29,67]. The non-parametric trend analysis revealed a changing trend of the NDVI3g from decreasing (browning) trends across a wider part of ADM, except over grass landscapes in which the NDVI3g showed significant increasing (greening) trends largely across the entire landscapes. Both the increased and decreased NDVI3g showed a statistically insignificant biogeophysical relationship with the climatic variables under investigation. The results revealed different patterns and fluctuations between the NDVI3g and the temperature, precipitation, solar radiation and wind speed (Figure S5). As a result, the increased (decreased) NDVI3g was linked to a decreasing (increasing) insignificant positive trend in temperature/radiation and subsequently increased (decreased) the precipitation as the length of the period increased. A recent study further corroborates the findings of these results based on NDVI trends and precipitation variations over the study area [28]. The results of vegetation dynamics with different climatic factors identified in this study differed seasonally and are broadly consistent with results of previous studies [28,29,67–72]. The changes in the climatic conditions further induced changes in the lower and upper atmospheric conditions. The decreasing (increasing) vegetation cover in ADM can alter the surface energy balance and hydrological cycles, thus influencing the feedback mechanism of vegetation on global climate change.

Based on the results from the pixel-wise partial correlation analysis, the spatial and temporal trends between the seasonal NDVI3g and climatic variables showed that the wind speed was the most influential factor among other climatic variables influencing seasonal vegetation variation, especially for winter and spring in ADM. During winter, the spatial characteristics of the seasonal NDVI–wind speed trend appeared to follow a particular trend that might be described by some large-scale atmospheric systems. This might have negatively influenced vegetation production and trend as a result of the damage caused by strong winds [73,74]. Although, the relationship between the NDVI3g and the wind speed was generally weak and largely insignificant. A strong south easterly summer wind that blows along the west coast, causes the offshore flow of the ocean, which might have a large impact on vegetation dynamics among other environmental factors [75,76]. In contrast, the reduction in the wind strength over the study area might exert a positive effect on vegetation growth [77,78]. The findings of this study suggest that the positive (negative) processes of vegetation change with the wind speed could be a dominant factor in winter, which is a transition period from winter to spring in ADM. Moreover, the positive processes of vegetation change with the wind speed in winter proposed by this study could further influence soil moisture and water availability as well as ecosystem functioning. The identified wind speed characteristics help to better understand the contribution of each season to the changes in spatial and seasonal characteristics of NDVI3g climatology and

the relationship between vegetation types and climate interactions in ADM. Several studies have revealed the importance of surface wind conditions in global climate system [77–79]. The identified positive correlation between the NDVI3g and the wind speed in all vegetation landscapes particularly in winter was based on remotely sensed vegetation data and other climatic variables from the ERA5-Land reanalysis data using various statistical methods. Nevertheless, a detailed study of feedback mechanisms based on an idealised simulation of a coupled vegetation-climate model is needed to identify more robust relationships between the vegetation activity and the climate in ADM. In addition, future investigations using observational data rather than reanalysis data are needed to fully understand the role of vegetation change on simulated vegetation-climate interactions and feedbacks in ADM. The newest GIMMS NDVI3g spatial resolution used for this study was relatively coarse, thus revealing overall trends for the entire ADM, but may not have enough resolution to accurately separate ecological processes. Therefore, future studies may use a higher spatial resolution dataset to better characterise vegetation trends and disentangle the impacts of external factors on vegetation change such as drought, warming, urbanization and ecological restorations.

5. Conclusions

In this study, pixel-wise partial correlation coefficient and non-parametric trend analyses were used to explore the NDVI3g for different seasons and different vegetation types and associated driving factors using long time-series remote sensing data from GIMMS (NDVI3g). The main conclusions of the study were summarised as follows. Firstly, during the 35 years from 1981 to 2015, the relationships between the NDVI3g and the climatic variables were relatively low ($R < 0.5$) and largely insignificant across vegetation types and seasons. The results somewhat suggested the potential role of atmospheric variations in vegetation changes in ADM. The large strength in inter-annual variation in the seasonal NDVI3g climatology and trends was observed in autumn and winter seasons with the highest productivity in these areas. The spatial and temporal trends in the NDVI3g peaked in the northwestern area majorly dominated by grassland/or shrubland and decreased towards the northeastern area of the region, where forest cover and/or crop landscape is predominant. Secondly, the correlation coefficient between the NDVI3g and the wind speed showed a stronger influence as a major driver of vegetation variation compared to other climate variables but was insignificant across the landscapes and seasons. Therefore, the wind as an essential climate component can affect carbon fluxes by changing carbon uptake and emission rates and also transport moisture and temperature from one area to another. Nevertheless, the impact of the wind speed has not received full attention in previous studies, thus assessing the characteristics of the variation of seasonal vegetation responses to the wind speed in the study area are crucial for sustainable forest resource utilization and ecological restoration. In general, the spatial and seasonal characteristics of the NDVI3g climatology in ADM indicated positive vegetation changes (increase) and vegetation types for the analysis period. Thirdly, the correlation coefficient between the NDVI and the climatic variables revealed an overall fluctuation across the seasons for different vegetation types with the largest decline in shrubs and/or crop landscape in these areas. This might be linked to the intended improvements on vegetation cover by the government which has not been fully undertaken in ADM, because the issues with the land use and land cover change and over-cultivation are yet to be fully resolved at the national level.

The deductions from this study are fundamental in designing strategies for targeted effective adaptation and mitigation to achieve sustainable vegetation and forest resource management. Uncertainties in terrestrial vegetation responses to future climate change require appropriate strategies to respond to climate issues and mechanistic approaches using remote sensing and GIS in light of the current result to address global change. This study suggests more studies on the assessment of ENSO impacts on spatiotemporal vegetation dynamics during the austral summer season to determine the degree and

extent of vegetation response to ENSO warm events. In addition, there is a need to use actual biophysical variables such as LAI to assess vegetation changes to validate remotely sensed trends. This will reveal useful information on the use of different data such as remote sensing indices to assess El Niño impact on vegetation cover for effective vegetation monitoring and assessment.

Supplementary Materials: The following supporting information can be downloaded at: <https://www.mdpi.com/article/10.3390/atmos13040620/s1>, Figure S1: Spatial characteristics of seasonal ERA5-Land 2m temperature climatology and trend (1981–2015) for ADM; Figure S2: Spatial characteristics of seasonal ERA5-Land precipitation climatology and trend (1981–2015) for ADM; Figure S3: Spatial characteristics of seasonal ERA5-Land shortwave radiation downward climatology and trend (1981–2015) for ADM; Figure S4: Spatial characteristics of seasonal ERA5-Land wind speed climatology and trend. (1981–2015) for ADM; Figure S5: Time-series of NDVI3g and climate variables from 1981 to 2015 for ADM.

Author Contributions: Conceptualisation, G.A.A.; methodology, G.A.A.; writing—original draft preparation, G.A.A.; writing—review and editing, K.A.I.; supervision, A.M.K. and I.R.O. All authors have read and agreed to the published version of the manuscript.

Funding: This research received funding from Govan Mbeki Research and Development Centre; (GMRDC): University Fort Hare, Alice, Eastern Cape Province, South Africa.

Institutional Review Board Statement: Not applicable.

Informed Consent Statement: Not applicable.

Data Availability Statement: Data used in this study are available on request. Requests for access to these data should be made to Gbenga Abayomi Afuye: afuyeabayomi@gmail.com.

Acknowledgments: The authors are grateful to the University of Fort Hare, South Africa for creating an enabling environment for research and to the anonymous reviewers for their wonderful insights that strengthened this paper.

Conflicts of Interest: The authors declare no conflict of interest.

References

1. Meng, X.H.; Evans, J.P.; McCabe, M.F. The impact of observed vegetation changes on land–atmosphere feedbacks during drought. *J. Hydrometeorol.* **2014**, *15*, 759–776. [[CrossRef](#)]
2. Miralles, D.G.; Gentile, P.; Seneviratne, S.I.; Teuling, A.J. Land–atmospheric feedbacks during droughts and heatwaves: State of the science and current challenges. *Ann. N. Y. Acad. Sci.* **2019**, *1436*, 19–35. [[CrossRef](#)] [[PubMed](#)]
3. Bright, R.M.; Zhao, K.; Jackson, R.B.; Cherubini, F. Quantifying surface albedo and other direct biogeophysical climate forcings of forestry activities. *Glob. Chang. Biol.* **2015**, *21*, 3246–3266. [[CrossRef](#)] [[PubMed](#)]
4. Duveiller, G.; Hooker, J.; Cescatti, A. The mark of vegetation change on Earth’s surface energy balance. *Nat. Commun.* **2018**, *9*, 12. [[CrossRef](#)]
5. Alkama, R.; Cescatti, A. Biophysical climate impacts of recent changes in global forest cover. *Science* **2016**, *351*, 600–604. [[CrossRef](#)]
6. Li, J.; Tam, C.Y.; Tai, A.P.; Lau, N.C. Vegetation–heatwave correlations and contrasting energy exchange responses of different vegetation types to summer heatwaves in the Northern Hemisphere during the 1982–2011 period. *Agric. For. Meteorol.* **2021**, *296*, 108208. [[CrossRef](#)]
7. Qu, M.; Hamdani, S.; Bunce, J.A. The physiology and genetics of stomatal adjustment under fluctuating and stressed environments. *Appl. Photosynth. New Prog.* **2016**, *3*, 30.
8. Driesen, E.; Van den Ende, W.; De Proft, M.; Saeys, W. Influence of environmental factors light, CO₂, temperature, and relative humidity on stomatal opening and development: A review. *Agronomy* **2020**, *10*, 1975. [[CrossRef](#)]
9. Boisvenue, C.; Running, S.W. Controls on provisioning services and forest productivity: Responses and risk under changing environmental conditions. *Nat. Clim. Chang.* **2013**, *11*, 129–149.
10. Afuye, G.A.; Kalumba, A.M.; Orimoloye, I.R. Characterisation of vegetation response to climate change: A review. *Sustainability* **2021**, *13*, 7265. [[CrossRef](#)]
11. Pearson, R.G.; Phillips, S.J.; Loranty, M.M.; Beck, P.S.; Damoulas, T.; Knight, S.J.; Goetz, S.J. Shifts in Arctic vegetation and associated feedbacks under climate change. *Nat. Clim. Chang.* **2013**, *3*, 673–677. [[CrossRef](#)]
12. Latella, M.; Bertagni, M.B.; Vezza, P.; Camporeale, C. An integrated methodology to study riparian vegetation dynamics: From field data to impact modeling. *J. Adv. Model. Earth Syst.* **2020**, *12*, e2020MS002094. [[CrossRef](#)] [[PubMed](#)]
13. Eamus, D.; Huete, A.; Yu, Q. *Vegetation Dynamics*; Cambridge University Press: New York, NY, USA, 2016.

14. Afuye, G.A.; Kalumba, A.M.; Busayo, E.T.; Orimoloye, I.R. A bibliometric review of vegetation response to climate change. *Environ. Sci. Pollut. Res.* **2021**, *25*, 1–3. [[CrossRef](#)] [[PubMed](#)]
15. Diaz, S.; Hector, A.; Wardle, D.A. Biodiversity in forest carbon sequestration initiatives: Not just a side benefit. *Curr. Opin. Environ. Sustain.* **2009**, *1*, 55–60. [[CrossRef](#)]
16. Osterkamp, W.R.; Hupp, C.R.; Stoffel, M. The interactions between vegetation and erosion: New directions for research at the interface of ecology and geomorphology. *Earth Surf. Process. Landf.* **2012**, *37*, 23–36. [[CrossRef](#)]
17. Abbas, F.; Hammad, H.M.; Fahad, S.; Cerdà, A.; Rizwan, M.; Farhad, W.; Ehsan, S.; Bakhat, H.F. Agroforestry: A sustainable environmental practice for carbon sequestration under the climate change scenarios—A review. *Environ. Sci. Pollut. Res.* **2017**, *24*, 11177–11191. [[CrossRef](#)]
18. Swain, S.; Wardlow, B.D.; Narumalani, S.; Tadesse, T.; Callahan, K. Assessment of vegetation response to drought in Nebraska using Terra-MODIS land surface temperature and normalized difference vegetation index. *GIScience Remote Sens.* **2011**, *48*, 432–455. [[CrossRef](#)]
19. Pettorelli, N.; Chauvenet, A.L.; Duffy, J.P.; Cornforth, W.A.; Meillere, A.; Baillie, J.E. Tracking the effect of climate change on ecosystem functioning using protected areas: Africa as a case study. *Ecol. Indic.* **2012**, *20*, 269–276. [[CrossRef](#)]
20. Li, Z.; Huffman, T.; McConkey, B.; Townley-Smith, L. Monitoring and modelling spatial and temporal patterns of grassland dynamics using time-series MODIS NDVI with climate and stocking data. *Remote Sens. Environ.* **2013**, *138*, 232–244. [[CrossRef](#)]
21. Kalisa, W.; Igbawua, T.; Henchiri, M.; Ali, S.; Zhang, S.; Bai, Y.; Zhang, J. Assessment of climate impact on vegetation dynamics over East Africa from 1982 to 2015. *Sci. Rep.* **2019**, *9*, 120. [[CrossRef](#)]
22. Wang, H.; Sun, B.; Yu, X.; Xin, Z.; Jia, G. The driver-pattern-effect connection of vegetation dynamics in the transition area between semi-arid and semi-humid northern China. *Catena* **2020**, *194*, 104713. [[CrossRef](#)]
23. Parida, B.R.; Pandey, A.C.; Patel, N.R. Greening and browning trends of vegetation in India and their responses to climatic and non-climatic drivers. *Climate* **2020**, *8*, 92. [[CrossRef](#)]
24. Muir, C.; Southworth, J.; Khatami, R.; Herrero, H.; Akyapı, B. Vegetation Dynamics and Climatological Drivers in Ethiopia at the Turn of the Century. *Remote Sens.* **2021**, *13*, 3267. [[CrossRef](#)]
25. Zhang, J.; Stegall, S.T.; Zhang, X. Wind–sea surface temperature–sea ice relationship in the Chukchi–Beaufort Seas during autumn. *Environ. Res. Lett.* **2018**, *13*, 034008. [[CrossRef](#)]
26. Piao, S.; Friedlingstein, P.; Ciais, P.; Zhou, L.; Chen, A. Effect of climate and CO₂ changes on the greening of the Northern Hemisphere over the past two decades. *Geophys. Res. Lett.* **2006**, *33*, 23. [[CrossRef](#)]
27. Murungweni, F.M.; Mutanga, O.; Odiyo, J.O. Rainfall trend and its relationship with normalized difference vegetation index in a restored semi-arid wetland of South Africa. *Sustainability* **2020**, *12*, 8919. [[CrossRef](#)]
28. Dyosi, M.; Kalumba, A.M.; Magagula, H.B.; Zhou, L.; Orimoloye, I.R. Drought conditions appraisal using geoinformatics and multi-influencing factors. *Environ. Monit. Assess.* **2021**, *193*, 19. [[CrossRef](#)]
29. Liu, H.; Song, X.; Wen, W.; Jia, Q.; Zhu, D. Quantitative Effects of Climate Change on Vegetation Dynamics in Alpine Grassland of Qinghai-Tibet Plateau in a County. *Atmosphere* **2022**, *13*, 324. [[CrossRef](#)]
30. Amathole District Municipality Integrated Development Plan Amathole District Municipality Integrated Development Plan 2011/2012—Version 5 of IDP 2011–2012. Available online: <http://www.amathole.gov.za/index.php/library2/shortcodes/headings-2/707-2011-12-idp.2012.2011/12> (accessed on 6 May 2020).
31. Graw, V.; Ghazaryan, G.; Dall, K.; Delgado Gómez, A.; Abdel-Hamid, A.; Jordaan, A.; Piroška, R.; Post, J.; Szarzynski, J.; Walz, Y.; et al. Drought dynamics and vegetation productivity in different land management systems of Eastern Cape, South Africa—A remote sensing perspective. *Sustainability* **2017**, *9*, 1728. [[CrossRef](#)]
32. Amathole District Municipality Wetland Report. Local Action for Biodiversity (LAB): Wetland Management in a Changing Climate, South Africa. Available online: https://africa.iclei.org/wp-content/uploads/2020/01/2017_Report_LAB_Amathole-district-municipality-wetland-report.pdf (accessed on 20 June 2020).
33. Phiri, M. *Spatial and Temporal Assessment of Vegetation Indices and Climatic Variables: The Case of Eastern Cape Province, South Africa*; University of Johannesburg: Johannesburg, South Africa, 2020.
34. Wang, J.; Rich, P.M.; Price, K.P. Temporal responses of NDVI to precipitation and temperature in the central Great Plains, USA. *Int. J. Remote Sens.* **2003**, *24*, 2345–2364. [[CrossRef](#)]
35. Wang, Y.; Roderick, M.L.; Shen, Y.; Sun, F. Attribution of satellite-observed vegetation trends in a hyper-arid region of the Heihe River basin, Western China. *Hydrol. Earth Syst. Sci.* **2014**, *18*, 3499–3509. [[CrossRef](#)]
36. StatsSSA. Statistics South Africa Community Survey. 2016. Available online: <http://www.statssa.gov.za/> (accessed on 20 August 2021).
37. SANBI. National Biodiversity Assessment. Available online: <http://bgis.sanbi.org/nba/project.asp> (accessed on 22 August 2021).
38. SANBI. Biodiversity Mainstreaming Toolbox for Land-Use Planning and Development in Gauteng. Compiled by ICLEI—Local Governments for Sustainability. 2014. Available online: http://biodiversityadvisor.sanbi.org/wp-content/uploads/2015/02/Biodiversity-Mainstreaming-Toolbox_Senior-Managers-Summary.pdf (accessed on 22 August 2021).
39. Nel, J.L.; Driver, A.; Strydom, W.F.; Maherry, A.; Petersen, C.; Hill, L.; Roux, D.J.; Nienaber, S.; Van Deventer, H.; Swartz, S.; et al. Atlas of Freshwater Ecosystem Priority Areas in South Africa. Available online: <https://www.fosaf.org.za/documents/SANBI/fish-priority-areas.pdf> (accessed on 7 July 2021).

40. Driver, A.; Sink, K.J.; Nel, J.L.; Holness, S.; Van Niekerk, L.; Daniels, F.; Jonas, Z.; Majiedt, P.A.; Harris, L.; Maze, K. National Biodiversity Assessment: An Assessment of South Africa's Biodiversity and Ecosystems. Available online: http://opus.sanbi.org/bitstream/20.500.12143/786/3/NBA2011_report.pdf (accessed on 8 July 2021).
41. Peres, C.A. Overharvesting. In *Conservation Biology for All*; Sodhi, N.S., Ehrlich, P.R., Eds.; Oxford University Press: New York, NY, USA, 2010.
42. Benhin, J.K. South African crop farming and climate change: An economic assessment of impacts. *Glob. Environ. Chang.* **2008**, *18*, 666–678. [[CrossRef](#)]
43. Amathole District Municipality. Climate Change Vulnerability Assessment and Response Framework. *Integr. Dev. Plan Rep.* **2011**, *11*, 1745.
44. Berliner, D.; Hayes, A.Y.; Desmet, P.; Hayes, R.; Berens, C. Eastern Cape Biodiversity Conservation Plan Handbook. Available online: https://www.dffe.gov.za/sites/default/files/docs/easterncapebiodiversity_conservationplan.pdf (accessed on 2 August 2021).
45. Mucina, L.; Rutherford, M.C.; Powrie, L.W.; Niekerk, A.V.; Van der Merwe, J.H. *Vegetation Field Atlas of Continental South Africa, Lesotho and Swaziland*; South African National Biodiversity Institute: Pretoria, South Africa, 2014.
46. Tucker, C.J.; Pinzon, J.E.; Brown, M.E.; Slayback, D.A.; Pak, E.W.; Mahoney, R.; Vermote, E.F.; El Saleous, N. An extended AVHRR 8-km NDVI dataset compatible with MODIS and SPOT vegetation NDVI data. *Int. J. Remote Sens.* **2005**, *26*, 4485–4498. [[CrossRef](#)]
47. Pinzon, J.E.; Tucker, C.J. A non-stationary 1981–2012 AVHRR NDVI3g time series. *Remote Sens.* **2014**, *6*, 6929–6960. [[CrossRef](#)]
48. Tong, S.; Zhang, J.; Bao, Y. Spatial and temporal variations of vegetation cover and the relationships with climate factors in Inner Mongolia based on GIMMS NDVI3g data. *J. Arid Land* **2017**, *9*, 394–407. [[CrossRef](#)]
49. Detsch, F. 'gimms v 1.2.1' R Package. Available online: <https://github.com/environmentalinformatics-Marburg/gimms> (accessed on 25 August 2021).
50. Dee, D.P.; Uppala, S.M.; Simmons, A.J.; Berrisford, P.; Poli, P.; Kobayashi, S.; Andrae, U.; Balmaseda, M.A.; Balsamo, G.; Bauer, D.P.; et al. The ERA-Interim reanalysis: Configuration and performance of the data assimilation system. *Q. J. R. Meteorol. Soc.* **2011**, *137*, 553–597. [[CrossRef](#)]
51. Hersbach, H.; Bell, B.; Berrisford, P.; Hirahara, S.; Horányi, A.; Muñoz-Sabater, J.; Nicolas, J.; Peubey, C.; Radu, R.; Schepers, D.; et al. The ERA5 global reanalysis. *Q. J. R. Meteorol. Soc.* **2020**, *146*, 1999–2049. [[CrossRef](#)]
52. Mechiche-Alami, A.; Abdi, A.M. Agricultural productivity in relation to climate and cropland management in West Africa. *Sci. Rep.* **2020**, *10*, 10. [[CrossRef](#)]
53. ESA. 2017. Available online: http://maps.elie.ucl.ac.be/CCI/viewer/download/ESACCI-LC-Ph2-PUGv2_2.0.pdf (accessed on 7 July 2021).
54. Jiang, W.; Yuan, L.; Wang, W.; Cao, R.; Zhang, Y.; Shen, W. Spatio-temporal analysis of vegetation variation in the Yellow River Basin. *Ecol. Indic.* **2015**, *51*, 117–126. [[CrossRef](#)]
55. Zhang, Y.; Ye, A. Quantitatively distinguishing the impact of climate change and human activities on vegetation in mainland China with the improved residual method. *GIScience Remote Sens.* **2021**, *58*, 235–260. [[CrossRef](#)]
56. Mann, H.B. Nonparametric tests against trend. *Econom. J. Econom. Soc.* **1945**, *11*, 245–259. [[CrossRef](#)]
57. Kendall, J.M. The turbulent boundary layer over a wall with progressive surface waves. *J. Fluid Mech.* **1970**, *41*, 259–281. [[CrossRef](#)]
58. Adeyeri, O.E.; Lawin, A.E.; Laux, P.; Ishola, K.A.; Ige, S.O. Analysis of climate extreme indices over the Komadugu-Yobe basin, Lake Chad region: Past and future occurrences. *Weather Clim. Extrem.* **2019**, *23*, 100194. [[CrossRef](#)]
59. Adeyeri, O.E.; Ishola, K.A. Variability and Trends of Actual Evapotranspiration over West Africa: The Role of Environmental Drivers. *Agric. For. Meteorol.* **2021**, *308*, 108574. [[CrossRef](#)]
60. Adeyeri, O.E.; Laux, P.; Ishola, K.A.; Zhou, W.; Balogun, I.A.; Adeyewa, Z.D.; Kunstmann, H. Homogenising meteorological variables: Impact on trends and associated climate indices. *J. Hydrol.* **2022**, *607*, 127585. [[CrossRef](#)]
61. Gu, Z.; Duan, X.; Shi, Y.; Li, Y.; Pan, X. Spatiotemporal variation in vegetation coverage and its response to climatic factors in the Red River Basin, China. *Ecol. Indic.* **2018**, *93*, 54–64. [[CrossRef](#)]
62. Liu, X.; Tian, Z.; Zhang, A.; Zhao, A.; Liu, H. Impacts of climate on spatiotemporal variations in vegetation NDVI from 1982–2015 in Inner Mongolia, China. *Sustainability* **2019**, *11*, 768. [[CrossRef](#)]
63. Zhu, M.; Zhang, J.; Zhu, L. Variations in growing season NDVI and its sensitivity to climate change responses to Green development in Mountainous areas. *Front. Environ. Sci.* **2021**, *9*, 179. [[CrossRef](#)]
64. Sen, P.K. Estimates of the regression coefficient based on Kendall's tau. *J. Am. Stat. Assoc.* **1968**, *63*, 1379–1389. [[CrossRef](#)]
65. Zemp, D.C.; Schleussner, C.F.; Barbosa, H.M.; Hirota, M.; Montade, V.; Sampaio, G.; Staal, A.; Wang-Erlandsson, L.; Rammig, A. Self-amplified Amazon forest loss due to vegetation-atmosphere feedbacks. *Nat. Commun.* **2017**, *8*, 10. [[CrossRef](#)] [[PubMed](#)]
66. Buras, A.; Rammig, A.; Zang, C.S. Quantifying impacts of the 2018 drought on European ecosystems in comparison to 2003. *Biogeosciences* **2020**, *17*, 1655–1672. [[CrossRef](#)]
67. Piao, S.; Wang, X.; Ciais, P.; Zhu, B.; Wang, T.A.; Liu, J.I. Changes in satellite-derived vegetation growth trend in temperate and boreal Eurasia from 1982 to 2006. *Glob. Chang. Biol.* **2011**, *17*, 3228–3239. [[CrossRef](#)]
68. Mohammad, A.; Wang, X.; Xu, X.; Peng, L.; Yang, Y.; Zhang, X.; Piao, S. Drought and spring cooling induced recent decrease in vegetation growth in Inner Asia. *Agric. For. Meteorol.* **2013**, *178*, 21–30. [[CrossRef](#)]

69. Liu, H.; Zhang, M.; Lin, Z.; Xu, X. Spatial heterogeneity of the relationship between vegetation dynamics and climate change and their driving forces at multiple time scales in Southwest China. *Agric. For. Meteorol.* **2018**, *256*, 10–21. [[CrossRef](#)]
70. Yao, R.; Wang, L.; Huang, X.; Chen, X.; Liu, Z. Increased spatial heterogeneity in vegetation greenness due to vegetation greening in mainland China. *Ecol. Indic.* **2019**, *99*, 240–250. [[CrossRef](#)]
71. Zhao, J.; Huang, S.; Huang, Q.; Wang, H.; Leng, G.; Fang, W. Time-lagged response of vegetation dynamics to climatic and teleconnection factors. *Catena* **2020**, *189*, 104474. [[CrossRef](#)]
72. Huang, J.; Ge, Z.; Huang, Y.; Tang, X.; Shi, Z.; Lai, P.; Song, Z.; Hao, B.; Yang, H.; Ma, M. Climate change and ecological engineering jointly induced vegetation greening in global karst regions from 2001 to 2020. *Plant Soil* **2021**, *29*, 120. [[CrossRef](#)]
73. Wahren, C.H.; Walker, M.D.; Bret-Harte, M.S. Vegetation responses in Alaskan arctic tundra after 8 years of a summer warming and winter snow manipulation experiment. *Glob. Chang. Biol.* **2005**, *11*, 537–552. [[CrossRef](#)]
74. Jiang, L.; Bao, A.; Guo, H.; Ndayisaba, F. Vegetation dynamics and responses to climate change and human activities in Central Asia. *Sci. Total Environ.* **2017**, *599*, 967–980. [[CrossRef](#)]
75. Shannon, L.V.; Nelson, G. The Benguela: Large scale features and processes and system variability. In *The south Atlantic*; Springer: Berlin/Heidelberg, Germany, 1996; pp. 163–210.
76. Niang, I.; Ruppel, O.C.; Abdrabo, M.A.; Essel, A.; Lennard, C.; Padgham, J.; Urquhart, P. Impacts, adaptation, and vulnerability. Part B: Regional aspects. Contribution of Working Group II to the fifth assessment report of the intergovernmental panel on climate change. *Afr. Clim. Chang.* **2014**, *11*, 1199–1266.
77. Jin, D.; Gao, Q.; Wang, Y.; Xu, L. Impacts of reduced wind speed on physiology and ecosystem carbon flux of a semi-arid steppe ecosystem. *Sciences* **2014**, *6*, 112.
78. Zhang, T.; Xu, X.; Jiang, H.; Qiao, S.; Guan, M.; Huang, Y.; Gong, R. Widespread decline in winds promoted the growth of vegetation. *Sci. Total Environ.* **2022**, *5*, 153682. [[CrossRef](#)] [[PubMed](#)]
79. Moustafa, M.; Wang, N. Assessment of wind and vegetation interactions in constructed wetlands. *Water* **2020**, *12*, 1937. [[CrossRef](#)]